Available online at www.sciencedirect.com
SCIENCE DIRECT®
JOURNAL OF CONSTRUCTIONAL STEEL RESEARCH
ELSEVIER Journal of Constructional Steel Research 59 (2003) 1101–1117
www.elsevier.com/locate/jcsr

Cross-frame and lateral bracing influence on curved steel bridge free vibration response

H. Maneetes, D.G. Linzell *

Department of Civil and Environmental Engineering, Pennsylvania State University, State College, PA 16802, USA

Received 4 September 2002; received in revised form 17 January 2003; accepted 12 February 2003

Abstract

Accurately quantifying the free vibration response of curved steel bridges has been a topic of interest for researchers and practitioners. This study examines the response of an experimental, single-span, noncomposite, curved I-girder bridge superstructure during free vibration. Finite element models of the experimental bridge system, which was tested for the FHWA Curved Steel Bridge Research Project (CSBRP), were constructed and calibrated against experimental data from dynamic investigations of the bridge by the Virginia Transportation Research Center (VTRC). Parametric studies of the experimental curved bridge system were conducted using these finite element models to investigate the effects of cross-frame and lateral bracing parameters on the structure's free vibration response.

Keywords: Curved bridge; Cross-frame; Lateral bracing; Free vibration; Construction; Finite element

1. Introduction

Horizontally curved bridges are commonly used in highway interchanges in large urban areas. Due to their curvature, the behavior of horizontally curved bridges is more complex than straight bridges. In addition to vertical shear and bending stresses present in straight girder systems, curved girders must also resist torsion that occurs due to curvature. So that these torsional effects can be effectively resisted by the curved girder system, both during construction and while in-service, cross-frames

* Corresponding author. Tel.: +814-863-8609; fax: +814-863-7304.
E-mail address: dlinzell@engr.psu.edu (D.G. Linzell).

0143-974X/03/$ - see front matter © 2003 Elsevier Science Ltd. All rights reserved.
doi:10.1016/S0143-974X(03)00032-4

between the girders must be designed as primary load resisting members and adequately distributed along the girder span.

In addition to the cross-frames, upper (near the plane of the girder top flange) and lower (near the plane of the girder bottom flange) lateral bracing may also be utilized. These lateral bracing components are generally provided to stabilize the curved girder system during construction by enhancing the torsional resistance of the system.

In general, there are few loads that are truly static in nature. Most loading that is of concern to the bridge designer is dynamic [12]. Dynamic loads not only occur while the bridge is in-service, but also during construction where they can result from equipment impact loads, impact and cyclical loads that occur when the deck is being placed (e.g. placement and consolidation of the concrete), or accidental vibrational loads. These loadings can lead to locked-in stresses and changes in the geometry of the bridge prior to it being placed into service that could alter its behavior from what is expected. Thus, understanding how curved steel bridges respond to free vibration during construction (i.e. before and while the deck is being placed) can help reduce stresses and displacements. Moreover, alignment problems that may result from costly construction delays could be minimized.

2. Background

Considerable research effort has been dedicated to studying the behavior of curved steel bridges in the United States during the past 10 years. The primary goal of this work has been to revise and improve existing design criteria for horizontally curved I-girder bridges.

The main experimental and numerical research project performed during this time period has been the Curved Steel Bridge Research Project (CSBRP), initiated by the Federal Highway Administration (FHWA) in 1992 [16]. This project has attempted to experimentally and analytically examine the behavior of curved steel I-girder bridges at full-scale to provide the necessary data that would be used to update and recalibrate the existing specifications. While the focal point of the CSBRP has been examining the behavior of various full-scale curved I-girder component sections under flexural, shear and combined flexural and shear loads, it has also incorporated limited full-scale testing during construction of a horizontally curved I-girder bridge in the laboratory, which served as a test frame for the component tests. Nine tests of six variations of the final framing plan of the bridge were completed and results were compared to analytical predictions from detailed ABAQUS finite element models. Results from these studies showed that the ABAQUS models accurately predicted behavior of the experimental bridge system during its construction [10]. In addition, limited experimental studies of the dynamic response were performed and data from those studies were used for the research described herein. The experimental structure and the dynamic tests that were performed will be described in detail in the sections that follow.

There have been a number of other studies of curved bridges completed during the past 20 years in addition to the recent large-scale research efforts. Some of that

work examined the affects of cross-frames on curved bridge response and is subsequently relevant to the study described herein.

Although they did not investigate dynamic response, Yoo and Littrell [14] performed finite element analyses of curved bridges with varying curvatures, lengths, and bracing intervals under truck live loads to develop an empirical equation for establishing maximum cross-frame spacing intervals. Results from the analyses were examined using linear and nonlinear regression techniques to predict the ratio of maximum bending stress, maximum warping stress, and maximum deck deflection for the curved bridge system to corresponding quantities for a straight bridge of equal length. A similar equation for establishing preliminary cross-frame spacing for curved steel I-girder bridges was developed through regression analysis by Davidson et al. [6]. Predictions from this equation were verified through additional finite element comparisons and comparisons to actual designs.

Yoon and Kang [15] investigated cross-frame effects on free vibration response for horizontally curved I-girder bridges with varying radii of curvature, cross-sections and number of cross-frames using the EQCVB program. It was observed that curved bridge frequencies were significantly affected by cross-frame stiffness. The effects of cross-frame variables on resulting stresses and deformations were not identified.

A few studies examining the influence of cross-frame members on straight bridge and curved bridge response under seismic loads have also been completed. The influence of cross-frames on the seismic performance of straight steel I-girder bridges was investigated by Azizinamini [5]. A two-span continuous composite bridge consisting of five haunched girders with two different types of cross-frames, X frames and K frames, was analyzed using SAP90. Cross-frame influence on maximum bottom flange lateral displacements, maximum moments developed in the webs, and maximum total base shears was examined. The studies showed that differences in behavior between X and K cross-frames were negligible.

Limited studies of lateral bracing systems in horizontally curved I-girder bridges have also performed. The effect of top and bottom lateral bracing on girder stress levels for single and continuous curved multigirder bridge systems was studied by Schelling et al. [13]. Results from the studies were in the form of equations that defined dead load distributions throughout the superstructure for the system both with and without lateral bracing. Multigirder bridges were also examined to determine the effect that placement of a concrete deck slab had on girder response with top and bottom lateral bracing. Heins and Jin [8] examined live load distribution considering the effects of lateral bracing for single and continuous curved composite I-girder bridges using a three-dimensional space frame formulation. Influences of bottom lateral bracing on load redistribution were considered and girder design equations were presented for use in conjunction with grid solutions or preliminary designs.

To date, only a single study has been performed that attempted to examine the effects of cross-frames and lateral bracing members on the response of curved steel bridges under dynamic loads. Keller [9] investigated the dynamic response of a system of horizontally curved steel I-girders for noncomposite dead load and composite live load conditions. The effects of span length, girder depth, number of girders, flange width, degree of curvature and cross-frame spacing were studied. It was found

that the addition of lateral bracing in curved I-girder bridges significantly improved the torsional rigidity of the system. The most influential parameter on curved I-girder dynamic behavior was found to be the degree of curvature, measured using either the L/R ratio or the girder subtended angle.

As the aforementioned summary indicates, there have been limited studies of the effects of cross-frames and bracing members on the dynamic response of curved bridges. The present study attempts to add to the state-of-the art by investigating the free vibration response of an experimental, single span, noncomposite, curved I-girder bridge during construction with varying cross-frame member cross-sections, geometries and spacings. It also studies the effects of lateral bracing position (i.e. near the plane of top flange or the bottom flange), orientation (i.e. placement of the bracing members in plan), and density (i.e. located in exterior bays only or in all bays) on response.

3. Experimental bridge

The experimental curved bridge initially tested for the CSBRP was composed of three simply supported curved steel I-girders braced radially using K-shaped cross-frames with radii of curvature of 58.3 m (191' 3"), 61.0 m (200' 0") and 63.6 m (208' 9"), respectively. Girder spans were 26.2 m (86' $0\frac{3}{4}''$), 27.4 m (90' 0") and 28.6 m (93' $11\frac{1}{4}''$) along the arc. Girder plate dimensions ranged between 1219.2 × 11.1 mm ($48''x\frac{7}{16}''$) and 1219.2 × 12.7 mm ($48''x\frac{1}{2}''$) for the webs and between 406.4 × 27.0 mm ($16''x1\frac{1}{16}''$) and 609.6 × 57.2 mm ($24''x2\frac{1}{4}''$) for the flanges. The K-type cross-frames consisted of 127.0 mm (5") diameter tubular members with a wall thickness of 6.4 mm ($\frac{1}{4}''$). Lower lateral bracing was used in the end panels of the exterior bays adjacent to the supports. A plan view of the bridge is shown in Fig. 1. The experimental bridge was proportioned so that failure would occur at midspan of G3 while the rest of the system remained elastic. Cross frames in the

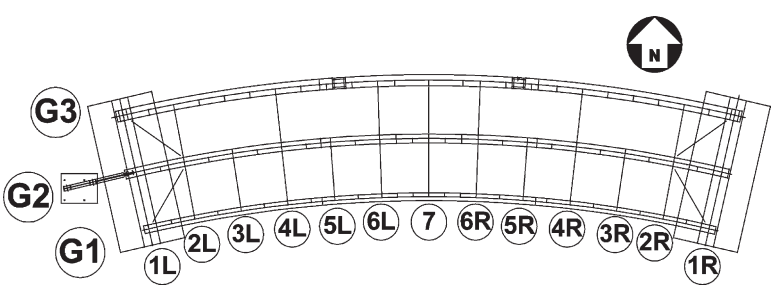

Fig. 1. Plan view of CSBRP experimental bridge [10].

vicinity of midspan spanned only between G1 and G2 and torsional moments subsequently increased near midspan of G3. The middle part of G3 was then designed to accommodate a number of different girder cross-sections so that their behavior could be examined. For the dynamic studies discussed herein, a section with properties equal to those for the remainder of G3 was spliced near midspan.

Vertical translation at the supports for G1 and G3 was restrained using spherical bearings. Teflon pads were provided to minimize tangential and radial frictional forces. G2 also utilized spherical bearings and Teflon pads, except that guided bearings were used to permit translation tangentially while restraining radial translation. Moreover, a pin placed in a vertically aligned slotted hole was used to connect a support frame tangent to the west end of G2 to prevent the entire system from slipping off the spherical bearings during testing.

4. Testing and instrumentation

The full-scale bridge free vibration test was completed by researchers from the Virginia Transportation Research Center (VTRC). The bridge was excited using a shaker positioned on the top flange at midspan of G3 as shown in Fig. 2. Nine accelerometers were positioned on the top and bottom flanges at midspan and the quarter span of the girders to capture their response in both the vertical and horizontal directions. Details of instrumentation used for the dynamic testing are shown in Fig. 3.

Accelerations were recorded at 0.005-s time increments for each test. Eight separate tests were performed and test time durations were between 150 and 300 s. Dominant natural frequencies of the structural system were found by converting acceleration signals from the time domain to the frequency domain by the Discrete Fourier Transform (DFT) technique using a Fast Fourier Transform (FFT) algorithm. The experimental natural frequency used for calibration was from the first dominant mode and had a magnitude of 2.90 Hz.

5. Finite element modeling

The finite element model used for the present parametric study was a variation of that utilized by Linzell [10], which was constructed in ABAQUS. All geometric, boundary and loading conditions were defined in a Cartesian coordinate system. The model consisted of approximately 8500 elements and 47 000 degrees of freedom. Shell elements were used to model the webs of all three girders and the flanges and stiffeners of G3. Beam elements were used to model girder flanges and stiffeners of G1 and G2 and all cross-frame and lateral bracing members. Solid elements were used to model splice plates that connected the plate girder specimens to the remainder of G3.

Restraint was provided in the vertical direction at the ends of all three girders. In addition to restraint in the vertical direction, radial and tangential translations were

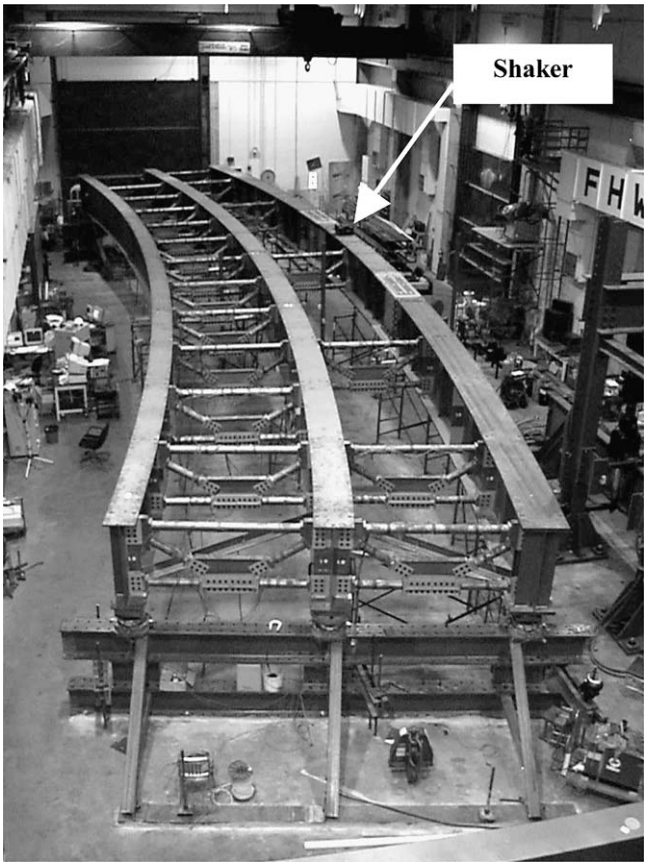

Fig. 2. End view of experimental bridge [10].

also restrained at the neutral axis near the west end of G2. Effects of the frame connected to G2's neutral axis were reproduced in the model using tangential and radial translational restraints. ABAQUS GAPUNI elements were used to model the Teflon bearings with an initial Coulomb frictional coefficient of 0.05. Nominal geometric and material properties were initially used for all components in the model. Loads applied to the model included self-weights of the bridge components and additional point masses that accounted for weights of connection details (e.g. gusset plates, connection plates) that were not explicitly modeled. The natural frequency of the first dominant mode had a magnitude of 3.87 Hz.

6. Model calibration

Data produced during testing of the experimental bridge consisted of vertical, tangential and radial accelerations only. Due to complexities involved with direct

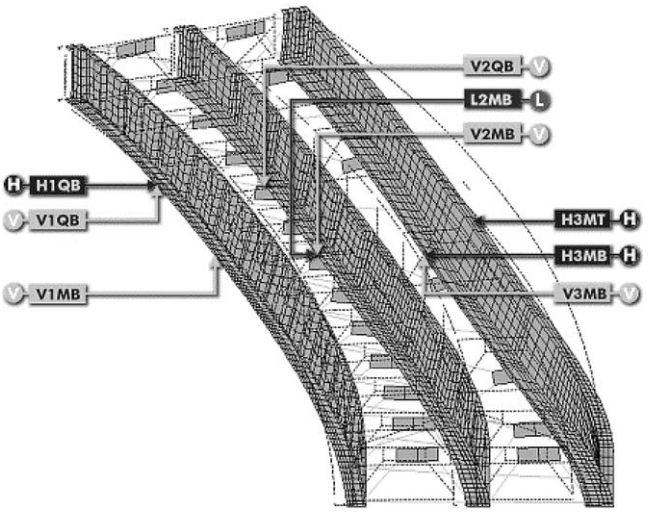

Fig. 3. VTRC instrumentation [11].

comparison between the data and the numerical model results, these accelerations were converted from the time domain to the frequency domain and calibration was performed by comparing experimental fundamental mode natural frequencies against fundamental frequencies produced from the analytical model. The experimental natural frequency against which comparisons were made was 2.90 Hz. The original finite element model gave a natural frequency of 3.87 Hz, which differed from the experimental results by 33%. To improve correlation between analytical results and experimental data, a number of items were reexamined and modified. These items included: boundary conditions, geometric properties, material properties and mass distribution. The final model used for the parametric studies was obtained by superimposing parameters that provided the most improvement during calibration. Effects of the various parameters on predicted response are summarized below.

6.1. Boundary conditions

Initial modification to the boundary conditions involved replacing the original assumed Coulomb friction coefficient with the values 0.01 and 0.10, which were selected from the viable range of friction coefficients for Teflon [7]. The studies showed that the effect of static friction on the results was negligible, with changes being less than 1%.

Continued examination of the influence of modifying the boundary conditions involved employing pins and horizontal rollers at the girder supports instead of the ABAQUS GAPUNI elements that were initially used. Accuracy of the natural frequency improved with horizontal rollers utilized at the ends, with a difference of 16% existing between analytical predictions and experimental results.

Contact surfaces were also introduced to attempt to better characterize the effect

of interaction of the Teflon pad with the bearing at the G2 supports. Contact pairs for G2 were defined using the ABAQUS small sliding algorithm [4]. Models utilizing contact surfaces at the supports gave results that were slightly better than those provided using simplified boundary conditions. However, differences between natural frequencies using contact surfaces with horizontal rollers and only horizontal rollers at the supports were quite small, being less than 0.1%. Since this difference was negligible, models utilizing horizontal rollers at the supports were selected for the parametric studies.

6.2. Geometric properties

The effects of varying geometric properties on natural frequencies predicted by the ABAQUS models were examined by replacing nominal dimensions with actual dimensions taken from measurements of the as-built structure [10]. Using measured dimensions had minor effects (less than 1%) on the predicted natural frequencies.

6.3. Material properties

To examine the effect of varying the material properties, elastic moduli for the steel components were modified from original nominal values to match results from coupon tests conducted during CSBRP testing [10]. Again, minor improvement in the analytical predictions (less than 1%) was demonstrated.

6.4. Mass distribution

In the original model, ABAQUS mass elements were used to include the effect of the weight of the large gusset plates used for cross-frame member connections (Fig. 2), which were not modeled explicitly to reduce the number of degrees of freedom. To examine the effect of distributing the gusset plate weight to more effectively match the actual distribution, extra nodes were generated in the region surrounding the gusset plates and additional concentrated mass loads were applied. When compared against the experimental data, results showed that the effect of revising these mass distributions on analytical natural frequencies was also negligible, being less than 0.1%.

6.5. Cumulative effects from calibration studies

A model was constructed that incorporated a combination of dominant parameters from the calibration studies. Analytical predictions from this model were then compared to the experimental data.

The first 10 modes from a modal analysis of the model that included modifications from the calibration studies were generated. The dominant analytical natural frequency, which corresponded to the maximum effective mass participation factor, was 2.46 Hz in the third mode. Experimental natural frequencies corresponding to this dominant mode were compared to analytical predictions and a difference of less than

15% existed. Given the size and complexity of the structure that was examined, the relatively coarse instrumentation scheme that was used, and simplifications that were made to reduce solution time, such as ignoring the connection details and performing linearly elastic small displacement analyses, this level of error was considered acceptable. The mode shape for the third mode is shown in Fig. 4.

7. Parametric study

7.1. General

A parametric study was conducted to examine the effects of various items on dynamic response utilizing the calibrated numerical model. Parameters that were examined included cross-frame geometry, cross-frame member cross-section, cross-frame spacing, lateral bracing position (i.e. near the plane of top flange or the bottom flange), lateral bracing orientation (i.e. orientation of the bracing members in plan), and lateral bracing density (i.e. located in exterior bays or in all the bays). Quantities that were studied under free vibration included natural frequencies, maximum vertical and lateral bending stresses, and maximum vertical and lateral displacements.

7.2. Cross-frame study

Details of the cross-frame parametric study cases are listed in Table 1. The two cross-frame types that were studied (K- or X-type) are commonly used for steel bridges in the United States. Member cross-sections that were examined provided similar axial stiffness properties as the original tubular members. Cross-frame spac-

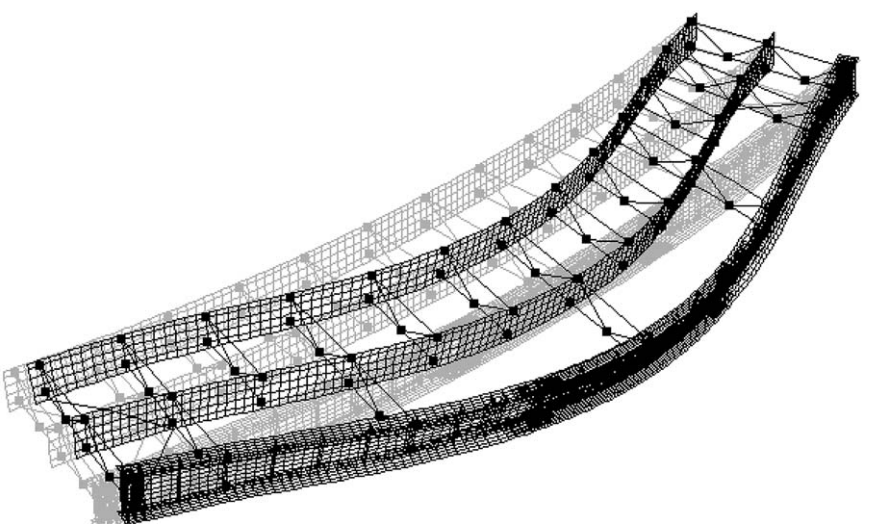

Fig. 4. Original and displaced structure, third mode.

Table 1
Cross-frame parameters

Item	Cross-frame shape	R/L ratio	Cross-frame cross-section
1	K-shaped	Upper bound	Tee (WT 6x15)
2		R/L = 13.33	Angle (L 6x6x3/8)
3		L = 4.57 m (15'-0")	Double Angles (2L's 3x3x3/8)
4			Pipe [127 mm (5") ∅ pipe]
5		Middle	Tee (WT 6x15)
6		R/L = 16.00	Angle (L 6x6x3/8)
7		L = 3.81 m (12'-6")	Double angles (2L's 3x3x3/8)
8			Pipe [127 mm (5") ∅ pipe]
9		Lower bound	Tee (WT 6x15)
10		R/L = 20.00	Angle (L 6x6x3/8)
11		L = 3.05 m (10'-0")	Double angles (2L's 3x3x3/8)
12			Pipe [127 mm (5") ∅ pipe]
13	X-shaped	Upper bound	Tee (WT 6x15)
14		R/L = 13.33	Angle (L 6x6x3/8)
15		L = 4.57 m (15'-0")	Double angles (2L's 3x3x3/8)
16			Pipe [127 mm (5") ∅ pipe]
17		Middle	Tee (WT 6x15)
18		R/L = 16.00	Angle (L 6x6x3/8)
19		L = 3.81 m (12'-6")	Double angles (2L's 3x3x3/8)
20			Pipe [127 mm (5") ∅ pipe]
21		Lower bound	Tee (WT 6x15)
22		R/L = 20.00	Angle (L 6x6x3/8)
23		L = 3.05 m (10'-0")	Double angles (2L's 3x3x3/8)
24			Pipe [127 mm (5") ∅ pipe]

ing intervals that were examined represented upper, middle and lower bound radii of curvature to unbraced length ratios (R/L) as specified by the AASHTO Guide Specifications [1] for horizontally curved steel bridges. The effect of each of these parameters on natural frequencies, stresses and displacements developed in the curved girder bridge system model were examined. Based on these studies, parameters influencing the response of the system were identified. Results are discussed below.

7.2.1. Cross-frame type

Natural frequencies for X-type cross-frames were shown to be 2% greater than frequencies obtained for K-type frames with the same member cross-section, which indicated that X-type cross-frames contributed more stiffness to the system than K-type cross-frames. However, X-type cross-frames weighed 29% more than similarly-sized K-type cross-frames and this weight had greater effects on maximum bending

stresses and displacements in the girders. Although higher natural frequencies were obtained for the X-type cross-frames, girder maximum vertical and lateral bending stresses and displacements were approximately 5% higher than those for K-type frames. The combination of these results indicated that, although certain parameters for X-type cross-frames were dominant when compared to those for K-type frames, the behavior of the two systems could be considered practically identical.

Tension flange midspan lateral bending stresses for K- and X-type cross-frames when the bridge was fully deflected under self-weight are illustrated in Fig. 5. Maximum compressive lateral bending stresses occurred at the inside flange tip while maximum tensile lateral bending stresses occurred at the outside tip. These plots indicate the negligible effect that cross-frame type had on response.

7.2.2. Cross-frame member cross-section

Cross-frames in curved bridge systems are designed as primary load-resisting members, and are subsequently proportioned to resist stresses generated due to axial, flexural and torsional forces. However, they are predominantly under axial and flexural loads. Thus, their axial and flexural resistances are the main cross-frame parameters that could affect the natural frequency. Since sections used for the parametric study had the same cross-sectional area, the single stiffness parameter considered was the major axis flexural stiffness for the different cross-sections. Strong axis moments of inertia for single tee, angle and pipe sections, which were 5.6×10^6 mm^4 (13.38 in^4), 6.4×10^6 mm^4 (15.34 in^4), and 6.3×10^6 mm^4 (15.20 in^4) respectively, were considerably greater than that for a double angle section, which was 1.5×10^6 mm^4 (3.52 in^4). Therefore, results from the parametric studies showed that tee, single angle, and pipe sections provided 8% higher natural frequencies than those for double angle cross-sections for both K- and X-type frames.

Although natural frequencies were marginally affected by cross-frame member

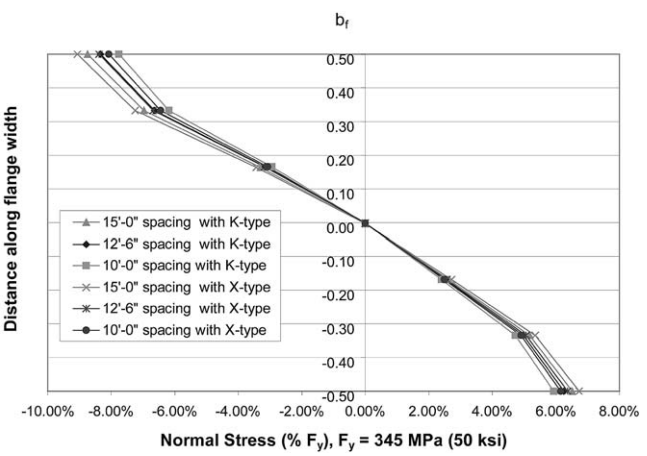

Fig. 5. Tension flange lateral bending stress variation at midspan G3, angle section.

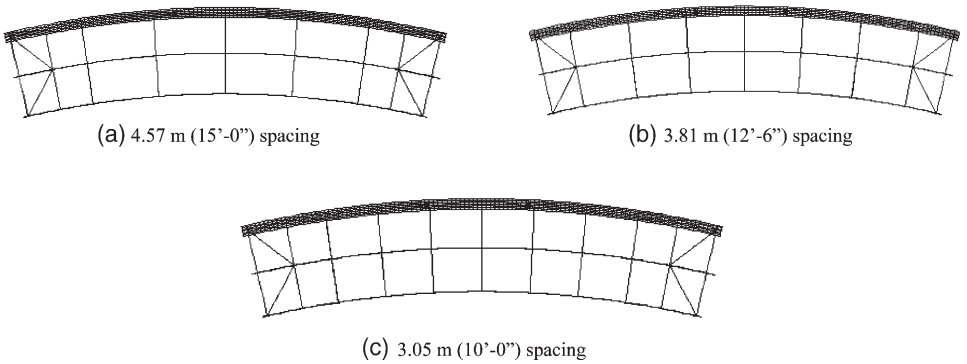

Fig. 6. Cross frame spacing parameters.

cross-sections, the effect of member cross-section on girder vertical bending stresses and displacements was negligible, being less than 1%.

7.2.3. Cross-frame spacing

Analyses were performed for varying cross-frame spacings. Note that when the 3.05 m (10' 0") spacing was used, additional cross-frames were added as illustrated in Fig. 6. The analyses show that vertical bending stresses and displacements tended to decrease with a reduction in cross-frame spacing for a system containing the same number of cross-frames [4.57 m (15' 0") and 3.81 m (12' 6") spacings] as shown in Fig. 7. The increase in the number of cross-frames with the 3.05 m (10' 0") spacing increased the system weight, which had an effect on natural frequencies and girder vertical bending stresses and displacements. The closer cross-frame spacing produced higher natural frequencies, which indicated that system with lower spacings was stiffer than systems with larger spacings. The range of increase in natural frequencies between the 4.57 m (15' 0") and 3.81 m (12' 6") spacings was between 0.8 and 1.4%. Natural frequencies for the 3.05 m (10' 0") spacing were almost equal to those obtained from 3.81 m (12' 6") spacing.

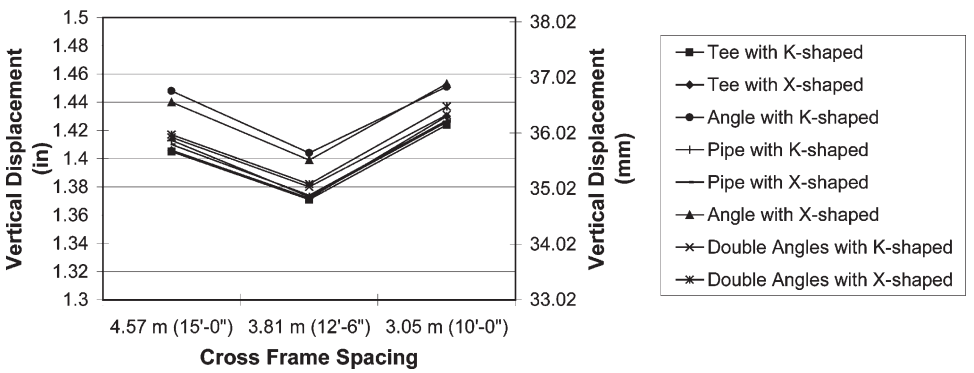

Fig. 7. Effect of cross-frame spacing on vertical displacement.

Due to the increased weight, the vertical bending stresses and displacements for the system with 3.05 m (10’ 0”) spacing were not significantly different from those of a system having a 4.57 m (15’ 0”) spacing. Fig. 7 indicates that vertical displacements obtained for a cross-frame spacing of 3.81 m (12’ 6”) are 3% less than displacements obtained for the cross-frames at 4.57 m (15’ 0”) spacing. However, when the cross-frame spacing changes to 3.05 m (10’ 0”), vertical displacements increase by 4% from the 3.81 m (12’ 6”) spacing and are 1% higher than the 4.57 m (15’ 0”) spacing. Lateral bending stresses and displacements were more heavily influenced by cross-frame spacing, irrespective of the number of cross-frames. Fig. 8 shows that decreases in lateral displacements over values obtained for 4.57 m (15’ 0”) spacing were 17 and 23% for 3.81 m (12’ 6”) and 3.05 m (10’ 0”) spacings, respectively. Corresponding decreases for X-type cross-frames were 19 and 24% for 3.81 m (12’ 6”) and 3.05 m (10’ 0”) spacings, respectively. Although these changes were large when examined as percentages, their magnitudes were still relatively small but not insignificant.

7.3. Lateral bracing

Lateral bracing parameters that were considered included:

- Bracing position: bracing members in the plane of the top flange or in the plane of the bottom flange.
- Bracing orientation: differing orientation of bracing members in plan.
- Bracing density: bracing in exterior bays only or bracing in all bays.

The effect of these parameters on response was studied by examining one cross-frame case, which was the analytical model containing X-type, Tee-shaped cross-sections with a 3.81 m (12’ 6”) spacing. Fig. 9 shows that nine lateral bracing placement pattern schemes were studied for this particular system. It should be noted that bracing patterns selected for the study were chosen using the original design orien-

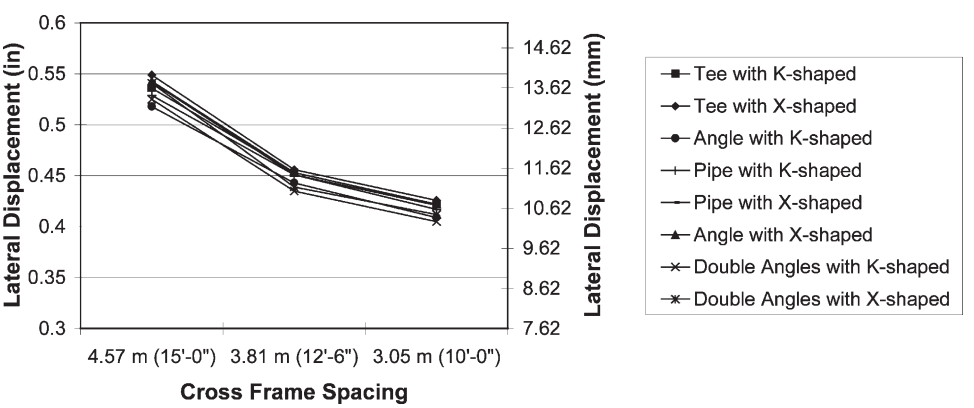

Fig. 8. Effect of cross-frame spacing on lateral displacement.

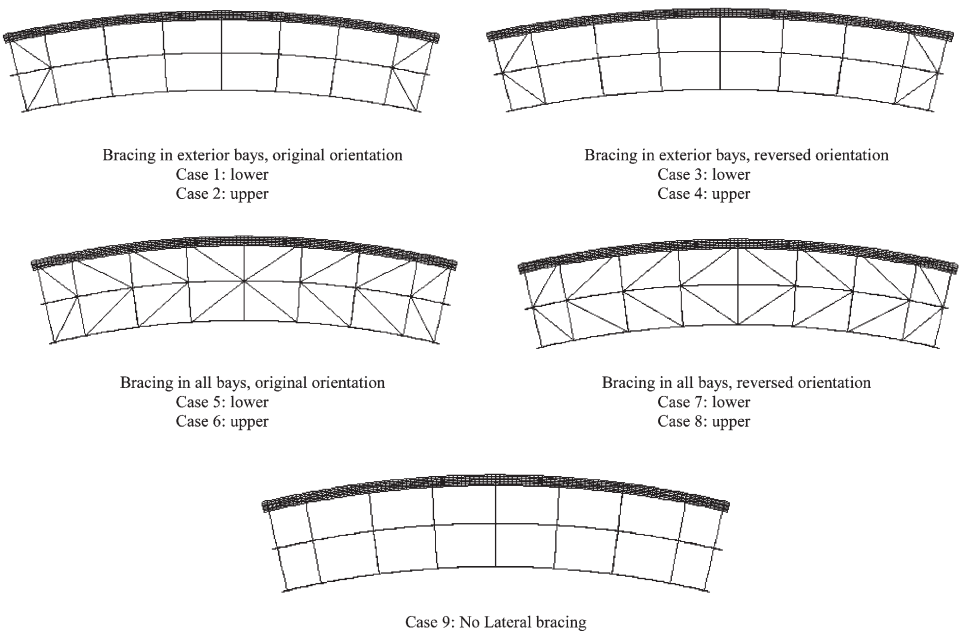

Fig. 9. Lateral bracing parameters.

tation for the exterior bays as a reference point (Fig. 1); they were not necessarily selected to reflect patterns commonly used in the field.

Lateral bracing location relative to the girder cross-section has an appreciable effect on vertical and lateral bending stresses. Results indicated that upper lateral bracing provided lower maximum vertical bending stresses than lower lateral bracing with differences approaching 6% for exterior bay lateral bracing and 13% for bracing in all bays. Maximum compressive lateral bending stresses at midspan of G3 followed the same trend. Lateral bending stresses were 48% lower for upper lateral bracing in exterior bays and 32% lower for upper lateral bracing in all bays when compared to systems containing similar lower lateral bracing arrangements, as illustrated in Figs 10 and 11. Though the percentage differences between these stresses are high, the magnitude of these differences is minimal.

There are no set criteria regarding the orientation of lateral bracing members in plan in AASHTO [1–3], hence orientations used for this study were those originally designed along with a scheme opposite to that originally used. Analytical results for natural frequencies were higher, with values increasing by a maximum of 9%, for the reversed bracing orientation scheme. These results indicated that the system having bracing oriented opposite to that originally used was stiffer when compared to the existing orientation. Lateral bracing orientation had minor effects on vertical bending stresses.

The number of lateral bracing members had a significant effect on natural frequency. Natural frequencies obtained for systems utilizing bracing members in all

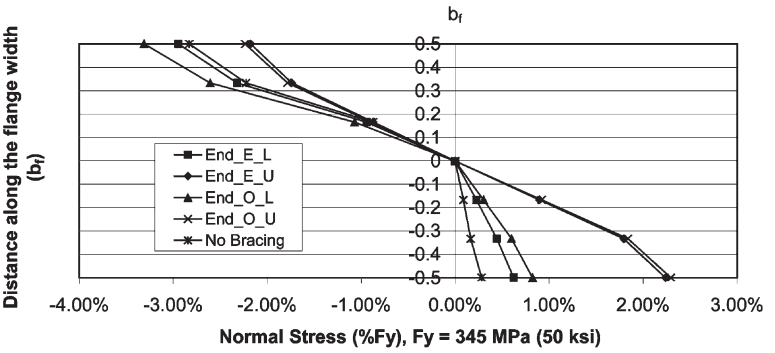

Fig. 10. Tension flange lateral bending stress variation at midspan G3, exterior bay lateral bracing.

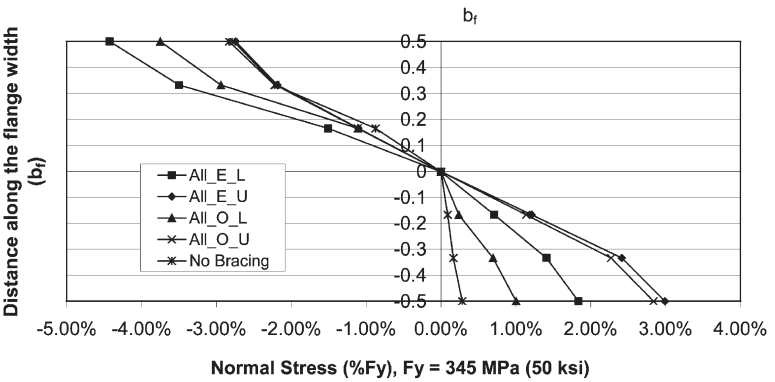

Fig. 11. Tension flange lateral bending stress variation at midspan G3, all bay lateral bracing.

bays were 57% higher than those with bracing members in the exterior bays and natural frequencies increased by 68% when lateral bracing was used in the exterior bays when compared to an unbraced system. Therefore, the effects of lateral bracing on system stiffness were significant even with bracing members located only in exterior bays. It was also observed that vertical bending stresses in the system with no lateral bracing were 15% higher than stresses in systems with lateral bracing in exterior bays. Moreover, the analytical model indicated that, for the system utilizing lateral bracing regardless of location, maximum bending stresses were spread over a smaller area when compared to the system with no lateral bracing.

8. Conclusions

This study provided valuable insight into the effect of various cross-frames and lateral bracing parameters on the free vibration response of the representative non-composite, curved, steel I girder bridge superstructure system. The parametric studies

helped identify influential parameters affecting dynamic response of the system. Identification of these parameters may, in turn, help with optimizing this structure or other similar structures to reduce their response.

Conclusions drawn from this research include:

- The combination of results from natural frequencies, stresses and displacements indicated that, for this structure, although certain parameters for X-type cross-frames were higher than those for K-type frames, the behavior of the two systems could be considered nearly identical.
- It appears that, for a structure of similar curvature, when vertical displacement is of concern, an increase in the number of cross-frames may prove to be uneconomical as there is not a corresponding increase in the efficiency of the system. However, when lateral displacement is of concern, an increased number of cross-frames would lead to a reduction in lateral displacements.
- When dynamic response is a concern, upper lateral bracing appeared to provide the most benefit for this structure and its use should be considered over part of the bridge length, especially when the curvature is sharp and the use of temporary supports is not practical.
- Lateral bracing orientation in plan had a negligible effect on vertical bending stress in this structure caused by self-weight.
- Bracing exterior bays of this structure led to a reduction in dynamic stresses and hence was more effective than an unbraced system. However, bracing in all bays did not lead to an appreciable reduction in dynamic stresses.

Acknowledgements

The authors would like to thank the Virginia Transportation Research Center for providing the experimental data used in this study and the Federal Highway Administration (FHWA) for allowing the authors access to the CSBRP experimental bridge.

References

[1] American Association of State Highway and Transportation Officials (AASHTO). Guide specifications for horizontally curved highway bridges, 1980: as Revised by Interim specification for bridges 1981, 1982, 1984, 1985 and 1986. Washington DC, 1993.
[2] American Association of State Highway and Transportation Officials (AASHTO). Standard specifications for highway bridges, Washington DC, 1993.
[3] American Institute of Steel Construction (AISC). Manual of Steel Construction, Load and Resistance Factor Design, Illinois, 1994.
[4] ABAQUS. ABAQUS user's manual. Hibbitt, Karlsson and Sorensen, 1998.
[5] Azizinamini A, Pavel R, Lotfi HR. Effect of cross bracing on seismic performance of steel I-girder bridges. In: Proceedings of Structures Congress XV: Building to Last, SEI-ASCE. 1996. p. 751–5.
[6] Davidson JS, Keller MA, Yoo CH. Cross-frame spacing and parametric effects in horizontally curved I-girder bridges. J Struct Engng, ASCE 1996;122(9):1089–96.
[7] Dupont. http://www.matweb.com/GetKeywordMatls.asp, 2001.

[8] Heins CP, Jin JO. Live load distribution on braced curved I-girders. J Struct Engng, ASCE 1984;110(3):523–30.
[9] Keller MA. Parametric study of horizontally curved I-girder systems including lateral bracing effects. MS thesis. Auburn, AL: Auburn University, 1994:97.
[10] Linzell DG. Studies of full-scale horizontally curved steel I-girder bridge system under self-weight. PhD dissertation. Atlanta, GA: Georgia Institute of Technology, 1999:710.
[11] Massarelli. Curved girder modal study: final instrumentation plan. http://www.people.virginia.edu/pjm8f/curve/final.html, 1998.
[12] Meyer C. Finite element idealization for linear elastic static and dynamic analysis of structures in engineering practice. New York: Task Committee on Finite Element Idealization, ASCE, 1987.
[13] Schelling D, Namini AH, Fu CC. Construction effects on bracing on curved I-girders. J Struct Engng, ASCE 1989;115(9):2145–65.
[14] Yoo CH, Littrell PC. Cross-bracing effects in curved stringer bridges. J Struct Engng, ASCE 1986;112(9):2127–40.
[15] Yoon K, Kang Y. Effects of cross beams on free vibration of horizontally curved I-girder bridges. In: Proceedings of the 1998 Annual Technical Session and Meeting, Structural Stability Research Council. 1998. p. 165–74.
[16] Zureick A, Naqib R, Yadlosky JM. Curved steel bridge research project, vol. 1. Interim Report (Synthesis), FHWA-RD-93-129, 1994:103.